

# Gas Pressure Sintering, Mechanical Properties and Microstructure of Three Kinds of $\text{Si}_3\text{N}_4$ Ceramics

Jung-Soo Ha, Chang-Sam Kim,<sup>\*†</sup> and Deock-Soo Cheong\*

School of Advanced Materials Engineering, Andong National University, Kyungbuk 760-749, Korea

<sup>\*</sup>Multifunctional Ceramics Research Center, Korea Institute of Science and Technology, Seoul 130-650, Korea

(Received July 6, 2004; Accepted August 26, 2004)

## ABSTRACT

Three kinds of  $\text{Si}_3\text{N}_4$  powders (M-11, SN-ESP, and SN-E10) were gas-pressure sintered at 1700 – 1900°C for 2 h under 18 atm  $\text{N}_2$ . Their densification behavior was investigated and compared as well as the mechanical properties and microstructure of the resulting ceramics. SN-ESP and SN-E10 started to reach nearly full densification at 1750°C and showed almost no decomposition up to 1900°C. In contrast, M-11 was not fully densified until 1800°C and showed about 3% weight loss at 1900°C indicating poor thermal stability. SN-ESP and SN-E10 showed much higher strength both at room temperature and 1200°C than M-11 when fully densified. Compared with SN-ESP, SN-E10 was not only a little better in strength (both at room temperature and 1200°C) and fracture toughness but also much higher in the Weibull modulus due to more interlocked microstructure by well elongated grains.

**Key words :**  $\text{Si}_3\text{N}_4$ , Gas pressure sintering, Densification behavior, Mechanical properties, Microstructure

## 1. Introduction

Due to the good mechanical, thermal, and chemical properties,  $\text{Si}_3\text{N}_4$  has wide applications such as cutting tools, ball bearings, mechanical seals, heat exchangers and various heat engine components. However, monolithic  $\text{Si}_3\text{N}_4$  shows the significant decrease in strength above 1200°C, which limits its high-temperature application.<sup>1-5)</sup>

One way to overcome this problem is to make  $\text{Si}_3\text{N}_4/\text{SiC}$  nanocomposites in which the matrix  $\text{Si}_3\text{N}_4$  is reinforced with SiC nano-sized particles.<sup>6-8)</sup> The nanocomposites exhibit significantly enhanced high-temperature strength and creep resistance compared with  $\text{Si}_3\text{N}_4$  monoliths. They are commonly fabricated by hot pressing to obtain a dense body of relative density of 99% or higher. In order to extend the application of the nanocomposites, Gas Pressure Sintering (GPS) is desirable because it allows complicate shapes, mass production and low cost.

In the present work, the GPS behavior of three kinds of  $\text{Si}_3\text{N}_4$  powders was investigated as a preliminary step to develop a fabrication process for the nanocomposites by GPS, along with the characterization of mechanical properties (strength at room temperature and 1200°C, hardness, fracture toughness, Weibull modulus) and microstructure.

## 2. Experimental Procedure

Three kinds of  $\text{Si}_3\text{N}_4$  powders selected in the present work were M-11 (H.C. Starck, Germany), SN-ESP (Ube Kosan, Japan), and SN-E10 (Ube Kosan, Japan).  $\text{Y}_2\text{O}_3$  (Johnson Matthey Co.) and  $\text{Al}_2\text{O}_3$  (AKP-30, Sumitomo Co.) were used as sintering aids. Table 1 shows the properties of the  $\text{Si}_3\text{N}_4$  powders. M-11 is made by a direct nitridation process, while SN-ESP and SN-E10 were made by an imide reduction method. The noteworthy differences between SN-ESP and SN-E10 are the average particle size and the specific

**Table 1.** Characteristics of  $\text{Si}_3\text{N}_4$  Powders Used

Grade	M-11	SN-ESP	SN-E10	
Manufacturer	H.C.Starck	Ube Kosan	Ube Kosan	
O	<1.5%	<2%	<2%	
C	<0.2%	<0.2%	<0.2%	
Al	<0.08%	<50 ppm	<50 ppm	
Impurities	Ca	<0.01%	<50 ppm	<50 ppm
	Fe	<800 ppm	<100 ppm	<100 ppm
	Mg	–	–	–
Cl	–	<100 ppm	<100 ppm	
Particle size distribution ( $\mu\text{m}$ )				
D 90	1.30	2.10	1.30	
D 50	0.60	0.70	0.50	
D 10	0.30	0.25	0.20	
$\alpha/(\alpha + \beta)$	>90%	>95%	>95%	
BET specific area ( $\text{m}^2/\text{g}$ )	12-15	6-8	9-13	

Corresponding author : Chang-Sam Kim

E-mail : cskim@kist.re.kr

Tel : +82-2-958-5483 Fax : +82-2-958-5489

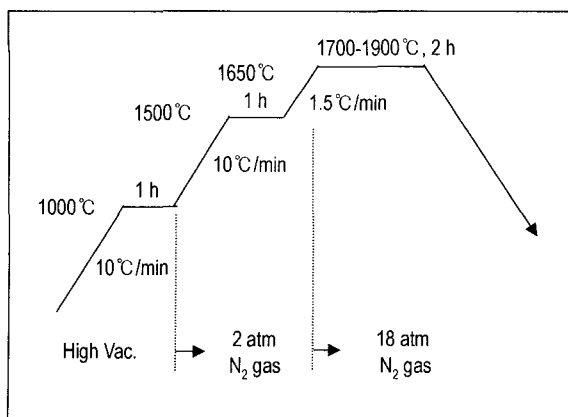


Fig. 1. Schedule of GPS.

surface area. SN-E10 has a smaller particle size and a larger specific surface area than SN-ESP.

The  $\text{Si}_3\text{N}_4$  powders were mixed with sintering aids of 7 wt%  $\text{Y}_2\text{O}_3$  and 4 wt%  $\text{Al}_2\text{O}_3$  by wet ball milling using  $\text{Si}_3\text{N}_4$  balls and jar for 24 h. The mixed powders were dried in an oven at 80°C for 24 h, and then sieved between 20 and 40 meshes for granulation. The granules were compacted uniaxially in a steel mold (25 × 50 mm) at 40 MPa and then isostatically pressed at 25000 psi. The green compacts were loaded into a graphite case coated with BN powder and sintered in a graphite furnace at  $\text{N}_2$  pressure of 18 atm. The GPS schedule is given in Fig. 1. The sintering temperature was varied between 1700 and 1900°C to find its effect on mechanical properties of sintered bodies and the soaking time at the sintering temperature was 2 h.

Weight losses of the samples were determined from the weights before and after sintering. Sintered densities were measured by the Archimedes method and converted to relative values to the theoretical density from a rule of mixture, obtained using the densities of  $\beta\text{-Si}_3\text{N}_4$  (3.19 g/cm<sup>3</sup>),  $\text{Al}_2\text{O}_3$  (3.98 g/cm<sup>3</sup>), and  $\text{Y}_2\text{O}_3$  (5.03 g/cm<sup>3</sup>). In order to characterize mechanical properties, the sintered bodies were machined and ground with diamond wheels (1500–2000 mesh) to give samples of 2 × 3 × 30 mm. Three-point bend tests were performed at room temperature and at 1200°C to evaluate fracture strength and Weibull modulus. The span was 20 mm and the cross head speed was 0.5 mm/min. The tensile surfaces of the samples were finished with 3  $\mu\text{m}$  diamond paste and the edges were beveled less than 0.1 mm with a diamond grinding wheel of 1200 grit. Weibull modulus was determined from the test results of more than 15 samples. Hardness was measured by the Vickers hardness test method, applying a full load of 10 kg<sub>f</sub> for 15 sec. Fracture toughness was estimated by the indentation fracture method using Evans and Charles equation.<sup>9)</sup> A full load of 20 kg<sub>f</sub> was applied for 15 sec and then the dimension of the diagonal depression and radial crack length in the indentation diagonals were used to calculate the fracture toughness. Microstructure of the samples was observed by Scanning Electron Microscopy (SEM) after plasma etching

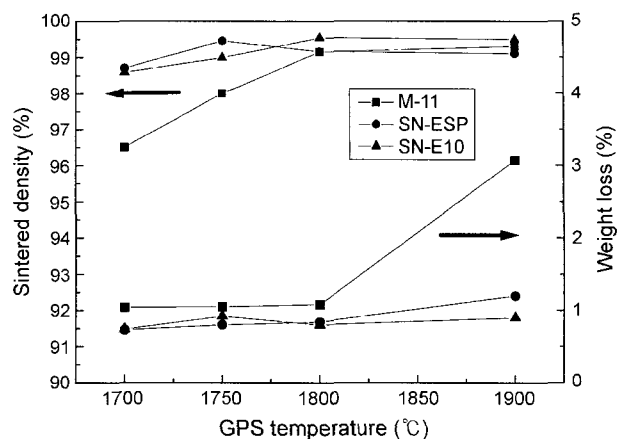


Fig. 2. Sintered density and weight loss as a function of GPS temperature.

to know the grain shape and size.

### 3. Results and Discussion

Fig. 2 shows densities and weight losses of sintered samples as a function of GPS temperature. SN-ESP and SN-E10 reached nearly full density at 1750°C and did not show any noticeable increases or decreases at higher temperatures. However, M-11 showed the maximum density at 1800°C, which was 50°C higher than for the others. Such a difference in the densification behavior is attributed to powder characteristics, because the sintering conditions such as soaking time, atmosphere and additives were same for all the three powders.

The characteristics of  $\text{Si}_3\text{N}_4$  powders influencing densification are primarily the specific surface area, particle size distribution and shape, and oxygen content. A higher specific surface area, a narrower particle size distribution and a certain amount of oxygen content generally accelerate densification and lower the densification temperature. On the other hand, a broad particle size distribution involving coarse particles inhibits densification by delaying the  $\alpha$ - $\beta$  phase transformation. Moreover, the coarse particles may leave large defects in sintered bodies, lowering the fracture strength.<sup>10,11)</sup>

SN-ESP and SN-E10 have a difference in the specific surface area and the particle size distribution (see Table 1). However, they showed nearly same densification behavior contrary to the general expectation mentioned above. On the other hand, M-11 has a higher specific surface area with a narrower or similar particle size distribution than or to SN-ESP and SN-E10. Nevertheless, it needed a higher temperature than the others to reach a full density. These facts suggest that the specific surface area and the particle size distribution were not the principal factors of densification in the present case. As shown in Table 1, M-11 is lower in the oxygen content compared with SN-ESP and SN-E10. Fig. 3 shows the morphology of M-11 and SN-E10 powders observed by SEM. It can be seen that many coarser particles

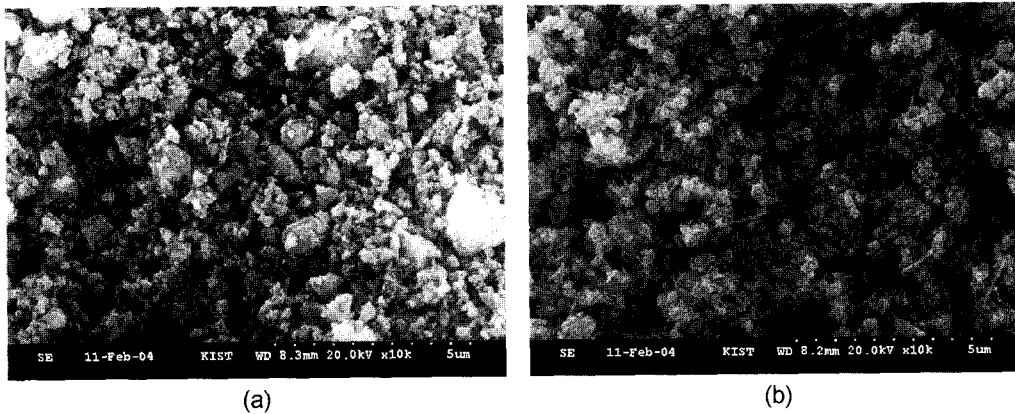


Fig. 3. SEM micrographs of (a) M-11 and (b) SN-E10 powders. Note the coarse grains as large as over  $1.5\ \mu\text{m}$  in (a).

( $1.5 - 2\ \mu\text{m}$  in diameter) were present in M-11 but not in SN-E10. Therefore, we can infer that the lower oxygen content and the presence of coarse particles in M-11 resulted in its lower densification behavior as compared with the other powders.

In Fig. 2, SN-ESP and SN-E10 did not show any weight loss change with the temperature, maintaining the values between 0.7 and 1.2%. Their ignition loss when heat-treated at  $1000^\circ\text{C}$  was 0.7%. Therefore it can be seen that SN-ESP and SN-E10 hardly decomposed up to  $1900^\circ\text{C}$ . In contrast, M-11 showed a larger weight loss about 3% at  $1900^\circ\text{C}$ , although it showed just slightly higher weight losses than SN-ESP and SN-E10 until  $1800^\circ\text{C}$ . Such good thermal stability of SN-ESP and SN-E10 must be a benefit when they are used for making silicon nitride based composites, which will need a sintering temperature as high as  $1900^\circ\text{C}$ .

Fig. 4 shows the strength at room temperature as a function of sintering temperature. SN-ESP and SN-E10 showed about 30% higher strength than M-11 with little difference between themselves. The fracture strengths of M-11 sintered below  $1750^\circ\text{C}$  were not measured due to their insufficient densities. Fig. 5 shows the strength at  $1200^\circ\text{C}$  as a

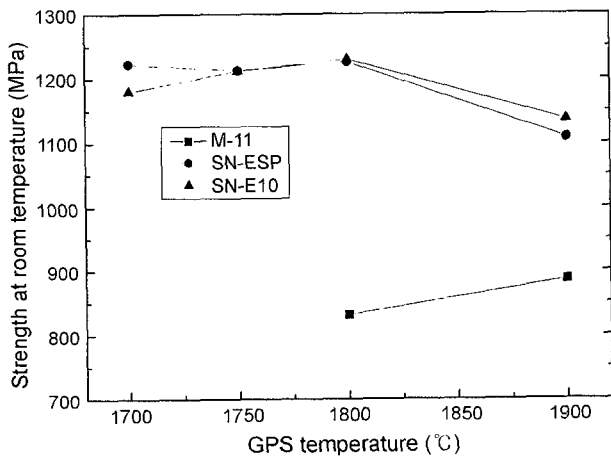


Fig. 4. Strength at room temperature as a function of GPS temperature.

function of sintering temperature. SN-ESP and SN-E10 were found to be also higher in high temperature strength than M-11, and SN-E10 exhibited better strength than SN-ESP. Fig. 6 shows the hardness and the fracture toughness of SN-ESP and SN-E10. Their hardness values were not noticeably different with a tendency to decrease with increasing the sintering temperature. The fracture toughness, on the contrary, had a tendency to increase with the

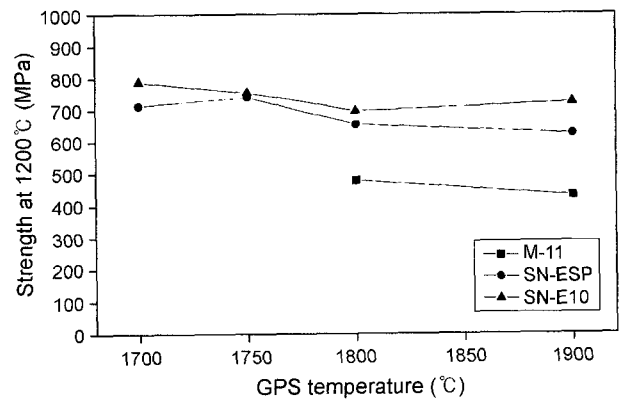


Fig. 5. Strength at  $1200^\circ\text{C}$  as a function of GPS temperature.

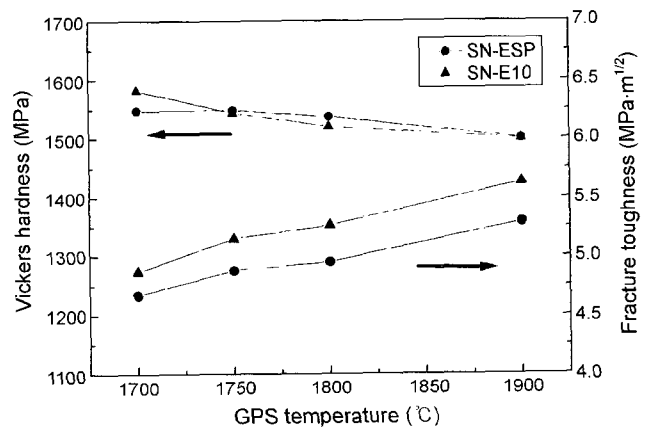
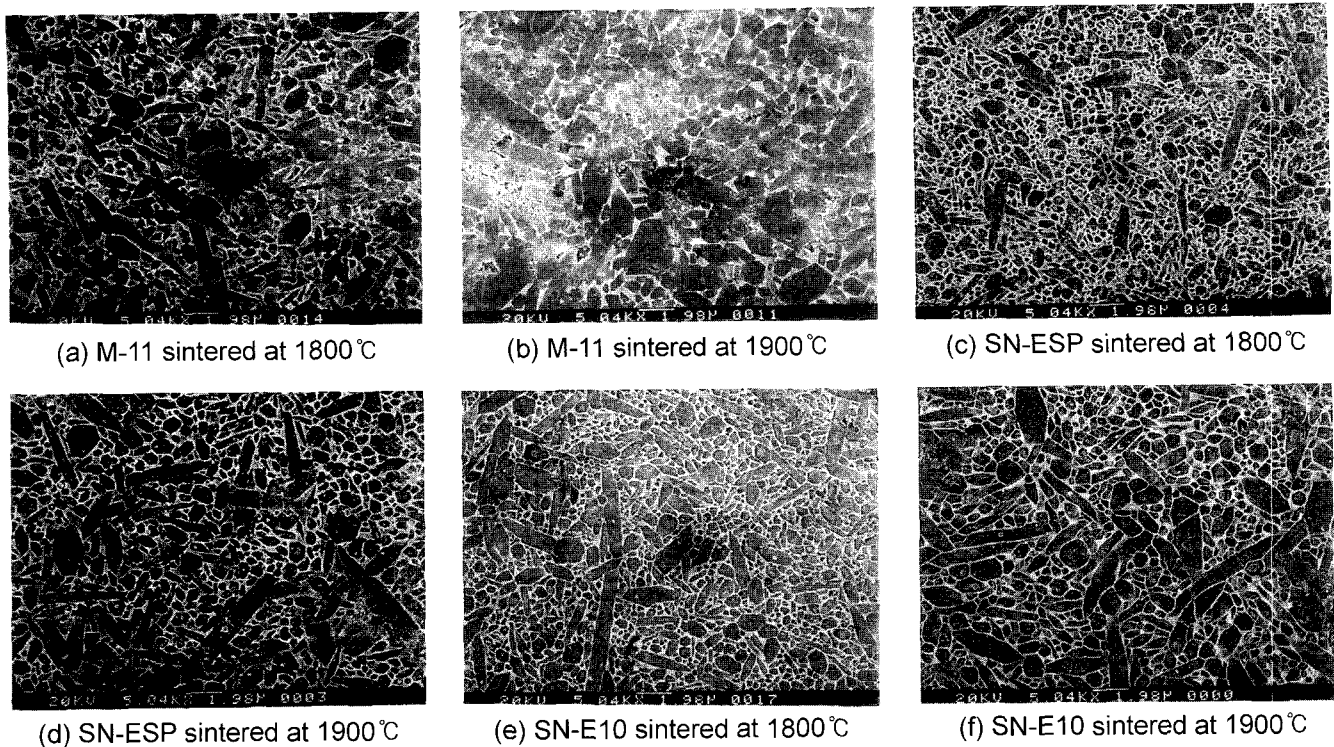


Fig. 6. Vickers hardness and fracture toughness as a function of GPS temperature.



**Fig. 7.** Scanning electron micrographs of etched surfaces of GPS samples : (a) M-11 sintered at 1800°C, (b) M-11 sintered at 1900°C, (c) SN-ESP sintered at 1800°C, (d) SN-ESP sintered at 1900°C, (e) SN-E10 sintered at 1800°C, and (f) SN-E10 sintered at 1900°C.

sintering temperature, and SN-E10 was better than SN-ESP like the high temperature strength.

Fig. 7 shows scanning electron micrographs of the etched surfaces of the GPS samples of the three powders, prepared at 1800 and 1900°C. With increasing sintering temperature, the grain size increased for all the specimens. M-11 had the largest grain size and the lowest aspect ratio, supporting the results of its weakest mechanical properties mentioned earlier. Under the same temperature, SN-E10 appeared to be a little larger than SN-ESP in the grain size and the aspect ratio. In silicon nitride ceramics, it is well known that a high aspect ratio contributes to fracture toughness and high temperature strength since it provides a strong interlocking of elongated grains. Therefore, it is attributed to these microstructural features that SN-E10 was better both in the strength at 1200°C (Fig. 5) and the fracture toughness (Fig. 6) than SN-ESP. One may suspect why the room-temperature strength was nearly same and even a little higher for SN-E10 for the GPS temperature of 1800°C and 1900°C, respectively (Fig. 4), although SN-E10 appeared to have slightly a larger grain size than SN-ESP (Fig. 7). This can be rationalized in terms of fracture toughness. That is, the higher fracture toughness of SN-E10 presumably counterbalanced or overcame the negative effect of the larger grain size on the strength.

Along with a strength, the Weibull modulus is an important parameter in the evaluation of mechanical properties of structural ceramics. It is a reliability parameter for

ceramic materials indicating a failure probability at a given stress. The general equation for determining the Weibull modulus is as follows:

$$P_f = 1 - \exp \left\{ - \int \left[ \frac{\sigma - \sigma_u}{\sigma_o} \right]^m dV \right\}$$

where  $P_f$  is the failure probability,  $\sigma$  the fracture stress,  $\sigma_u$  the stress for zero failure probability,  $\sigma_o$  the distribution parameter,  $m$  the Weibull modulus and  $V$  the specimen volume. The Weibull modulus data of SN-ESP and SN-E10 are given in Table 2 along with the strength values at room temperature. For M-11, there is no need to concern the Weibull modulus because of its poor properties in the thermal stability and strength (both at room temperature and 1200°C). It can be seen that SN-E10 showed much higher values than SN-ESP for the GPS temperatures 1800°C and 1900°C, which would be the temperatures required for  $\text{Si}_3\text{N}_4$  based nanocomposites to get dense bodies by GPS. The

**Table 2.** Weibull Moduli ( $m$ ) and Strength ( $\sigma_f$ ) of SN-ESP and SN-E10 GPS Samples at Room Temperature

GPS temperature (°C)	SN-ESP		SN-E10	
	$m$	$\sigma_f$ (MPa)	$m$	$\sigma_f$ (MPa)
1750	14	1213	13	1212
1800	16	1226	25	1230
1900	8	1108	17	1136

Weibull modulus decreased with 1900°C for both the powders probably due to the abnormal grain growth (Fig. 7). The Weibull modulus (25) and the strength (1230 MPa) obtained for SN-E10 with 1800°C were the highest. Considering the Weibull modulus and the other properties (i.e., densification, thermal stability, strength at room temperature and 1200°C, and fracture toughness), SN-E10 would be a better choice as the raw material for making the composites than the others.

#### 4. Conclusions

Three kinds of  $\text{Si}_3\text{N}_4$  powders (M-11, SN-ESP, and SN-E10) were compared on their GPS behavior and the mechanical properties and microstructure of the sintered ceramics as a preliminary step to find out the one suitable for making  $\text{Si}_3\text{N}_4$  based nanocomposites. SN-ESP and SN-E10 started to reach nearly full densities at 1750°C and showed almost no decomposition up to 1900°C. In contrast, M-11 needed 1800°C for the same densification due to its lower oxygen content and the presence of coarse particles in the powder. Moreover it showed a large weight loss about 3% at 1900°C indicating poor thermal stability. SN-ESP and SN-E10 showed much higher strength both at room temperature and 1200°C than M-11 when fully densified. Compared with SN-ESP, SN-E10 was not only a little better in strength (both at room temperature and 1200°C) and fracture toughness but also much higher in the Weibull modulus due to more interlocked microstructure by well elongated grains. It seems that SN-E10 is a good candidate as the raw material for making  $\text{Si}_3\text{N}_4$  based nanocomposites owing to its good properties in densification, thermal stability, mechanical properties and microstructure. Further studies are needed to demonstrate this speculation with making the composites.

#### REFERENCES

1. G. Ziegler, J. Heinrich, and G. Wotting, "Review: Relationships between Processing, Microstructure and Properties of Dense and Reaction-Bonded Silicon Nitride," *J. Mater. Sci.*, **22** 3041-86 (1987).
2. G. E. Gazza, "Effect of Yttria Additions on Hot-Pressed  $\text{Si}_3\text{N}_4$ ," *Ceram. Bull.*, **54** [9] 778-81 (1975).
3. D. A. Bonnel, T.-Y. Tien, and M. Ruhle, "Controlled Crystallization of the Amorphous Phase in Silicon Nitride Ceramics," *J. Am. Ceram. Soc.*, **70** [7] 460-65 (1987).
4. L. U. J. T. Ogbuji, "Role of  $\text{Si}_2\text{N}_2\text{O}$  in the Passive Oxidation of Chemically-Vapor-Deposited  $\text{Si}_3\text{N}_4$ ," *J. Am. Ceram. Soc.*, **75** [11] 2995-3000 (1992).
5. T. Ohji, S. Sakai, M. Ito, Y. Yamauchi, and W. Kanematsu, "Yielding Phenomena of Hot-Pressed  $\text{Si}_3\text{N}_4$ ," *High Temperature Tech.*, **5** [3] 139-44 (1987).
6. K. Niihara, "New Design Concept of Structural Ceramics; Ceramic Nanocomposites," *The Centennial Issue of the Ceramic Society of Japan, J. Ceram. Soc. Jpn.*, **99** [10] 974-82 (1991).
7. F. Wakai, Y. Kodama, S. Sakaguchi, N. Murayama, K. Izaki, and K. Niihara, "A Superplastic Covalent Crystal Composite," *Nature*, **344** 421-23 (1990).
8. G. Sasaki, H. Nakase, K. Suganuma, T. Fujita, and K. Niihara, "Mechanical Properties and Microstructure of  $\text{Si}_3\text{N}_4$  Matrix Composite with Nano-Meter Scale SiC Particles," *J. Ceram. Soc. Jpn.*, **100** [4] 536-40 (1992).
9. A. G. Evans and E. A. Charles, "Fracture Toughness Determination by Indentation," *J. Am. Ceram. Soc.*, **59** 7-8 (1976).
10. F. K. van Dijen, A. Kerber, U. Vogt, W. Pfeiffer, and M. Schulze, "A Comparative Study of Three Silicon Nitride Powders, Obtained Three Different Synthesis," *Key Eng. Mater.*, **89-91** 19-28 (1994).
11. T. Yamada, Y. Kanetsuki, K. Fueda, T. Takahashi, Y. Kohtoku, and H. Asada, "Effect of Powder Characteristics on Sintering Behavior of Silicon Nitride," *Key Eng. Mater.*, **89-91** 177-80 (1994).